SILVER NANOPARTICLES IN MONTMORILLONITE AND ANTIBACTERIAL ACTIVITY

[1]SHABNAM SOHRABNEZHAD, [2]AFSANEH SAIFI

[1,2]Department of Chemistry, Faculty of Science,
University of Guilan, P.O. Box 1914 Rasht. Iran.
E-mail: [1]sohrabnezhad@guilan.ac.ir

Abstract - The Ag-MMT nanocomposite, formed from $AgNO_3$/MMT suspension. $AgNO_3$ and Urtica dioica leaf extract were used as a silver precursor and reducing agent, respectively. The nanocomposite was characterized by x-ray diffraction (XRD), fourier transform infrared spectroscopy (FTIR), transmission electron microscopy (TEM), and UV-Vis spectroscopy. The XRD showed intercalation of Ag nanoparticles (Ag NPs) into the clay interlayer space. The UV-Vis indicated a strong surface plasmon resonance (SPR) absorption band in the UV region, resulting from metallic Ag NPs. The intensity of the SPR band increased with time in the $AgNO_3$/MMT suspension. But the results was opposite in case of Ag^+ solution. The stability of Ag NP in MMT was more than without support. These results showed that Ag NPs can be used as effective growth inhibitors in different biological systems.

Keywords - Montmorillonite; Surface plasmon resonance; nanocomposite; Biomaterials.

I. INTRODUCTION

Usually, nanoparticles show good antibacterial properties arising from their large surface area to volume ratio providing desirable contact with bacterial cell [1]. In recent years, metal nanoparticles based on silver [2], gold [3], copper [4] have been applied in medicine, dentistry, pharmacy, and biology. With increasing concerns about bacterial infections, there is a growing need to develop new and powerful antibacterial agents. Generally, nanoparticles can be produced through different methods among them; with chemical approaches are the most popular [5]. However, these methods cannot avoid the use of toxic chemicals in the synthesis protocol. Therefore, there is a growing need to develop eco-friendly processes for nanoparticles synthesis that do not use toxic chemicals. Biological methods of nanoparticles synthesis using microorganisms [6], enzymes [7], and plants or plant extracts [8] have been suggested as possible eco-friendly alternatives to chemical and physical methods. Using plants for nanoparticle synthesis can be advantageous over other biological processes such as microbial route, because it eliminates the elaborate process of maintaining cell cultures. For the synthesis of Ag NPs in the solid substrate, chemical and physical methods were often used. There is low data about biosynthesis of Ag NPs in supports by utilizing the aqueous leaves extract of plants. In this study *Urtica dioica* leaf extract was chosen as a reducing agent for the synthesis of Ag nanoparticles from $AgNO_3$ and $AgNO_3$/montmorillonite (MMT) suspension ($[Ag\text{-}MMT]^+$), separately. Urtica dioica, is a herbaceous perennial flowering plant and the leaves contain triterpenoids, alkaloids, polyphenols and tannins [9], hence this plant is chosen as reducing agent for the synthesis of Ag nanoparticles. The MMT was used as the protective colloid preventing the Ag NPs from aggregation. The antibacterial activities of the samples were investigated and compared with one another.

II. EXPERIMENTAL

The commercial sodium montmorillonite clay (NaMMT) was purchased from Southern Clay Products (Gonzales, TX). *Urtica dioica* leaves were collected from one of the cities around Tehran, Iran, and were cleaned with double distilled water. 10 g of this plant leaves were stirred with 100 ml de-ionized water at 60°C for 24 h, and filtered to get the extract. For synthesis of Ag nanoparticles in MMT, 1.0 mL of leaf extract was added to 2.0 mL of 1.0×10^{-2} M $AgNO_3$ and the volume was adjusted to 10 mL with double distilled water for the green reduction process. In order to establish the role of MMT in the green biosynthesis of Ag-nanoparticles, synthesis of Ag NPs was done in absence and presence of MMT. Gram-positive bacteria, ie, *Staphylococcus aureus* (*S.aureus*) and *Micrococcus lutes (M.lutes)* and Gram-negative bacteria, ie, *Escherichia coli (E. coli)*, *Pseudomonas aeruginosa (P. aeruginosa)*, were applied for antibacterial testing. The bacterial were obtained from the microbiology laboratory of Guilan University in the north Iran. For the determination of antibacterial activities of the prepared nanocomposites, well diffusion was used as described by Radhika et al. [10].

Powder X-ray diffraction patterns of the samples were recorded using an X-ray diffractometer (Bruker D8 Advance) with Co Kα radiation (λ = 1.789 A°). UV–Vis absorption spectra were recorded using a Shimadzu 1600 PC in the spectral range of 190-900 nm. The infrared spectra were measured on a Bruek spectrophotometer using KBr pellets. The transmission electron micrographs (TEM) were recorded with a Philips CM10 microscope, working at a 100 kV accelerating voltage.

III. RESULTS AND DISCUSSION

The XRD patterns of samples are shown in Fig. 1. The MMT matrix exhibited a 001 reflection with a d–value of 1.24 nm (8.25° 2θ) [11]. The XRD pattern of the Ag NPs showed A series of diffraction peaks at 37.52, 44.61 and 64.57º which are assigned to the silver nanoparticles (JCPDS No. 65-2871) [12]; and the diffraction peaks at 32.32, 37.52, 54.24 and 67.66º in the pattern of Ag NPs correspond to the cubic structure of Ag_2O (JCPDS No.41-1104) [13]. The XRD pattern for the Ag-MMT nanocomposite showed only the presence of metallic silver at 2θ = 37.56 and 44.77º. The reflection at 2θ = 8.25º for pure NaMMT, was shifted to 2θ = 7.89º, corresponding to a d-value of 1.29 nmin Ag-MMT. The increase of the distance between the layers could be attributed to the intercalation of Ag NPs into the clay layers.

The FT-IR spectra of MMT, Ag NPs and Ag–MMT samples showed the most intensive band at 1055 cm^{-1} which was attributed to Si–O in-plane stretching vibration. The OH-stretching band at 3631cm^{-1}, was due to hydroxyl group bonded with Al^{3+} cations [14]. Ag nanoparticles formed by reduction of Ag^+ ions showed FTIR bands at 3391 cm^{-1} (O–H vibration), 1638cm^{-1} (shifting of stretching band of C=O group), 1387 cm^{-1} (geminal methyls), and 1046 cm^{-1} (ether linkages). The FTIR data supported the presence of phenolic acid adsorbed on the surface of metal nanoparticles [9]. The Ag NPs formed by reduction of Ag^+ ions using *urtica dioica* leaf extract. The –OH group of phenolic compound in leaves of *urtica* may be responsible for the reduction of Ag^+ ions into metallic Ag [9]. All the bands related to phenolic acid in the Ag–MMT sample showed shift to higher wave numbers and intensity decreased compared to the Ag NPs. This confirmed the presence of nanosized the Ag NPs present in the MMT matrix.

For study of optical properties of samples, UV-Vis spectroscopy was used. The reaction mixture consisting of silver nitrate and $AgNO_3$/MMT suspension in *urtica* leaf extract separately, showed a color change from clear to a red color as the reaction proceeds. Within 15 min, the solution obtained, showed a deep red color. This reduction time is much faster than other methods [15, 16]. The results showed that the characteristic SPR band of the synthesized Ag NPs in absence and presence of MMT was at 370 nm. This band is due to the transverse plasmon vibrations [15]. As the reaction proceeds, the absorbance intensity at λ_{max} (370 nm) decreases and increases with time for the synthesized Ag NPs from Ag^+ solution and $[Ag\text{-}MMT]^+$ suspension with *urtica* leaf extract, respectively (Fig. 2). As the particles destabilize, the original absorption peak, due to the depletion of stable nanoparticles, will decrease in intensity. But Ag NPs were stable (even for month) into the clay interlayer space [17]. The SPR band was shifted to longer wavelengths and broadness in the absence and presence of stabilizer MMT when the concentration of silver ions was increased. The shifted and broadness, probably, is related to the Ag NPs diameter increases [17]. In high concentration of silver ions (10 mM), the silver nitrate and $[Ag\text{-}MMT]^+$ suspension in *urtica* leaf extract showed the SPR band in 410 and 395 nm respectively. These bands are due to the longitudinal plasmon vibrations [15].

TEM images of the samples are shown in Fig. 3. It was observed that the Ag NPs in absence of MMT (Fig. 3a) tended to agglomerate into clusters. The average size of Ag NPs was 30 nm. The obtained TEM images of the Ag NPs into the clay interlayer MMT (Fig. 3b) clearly indicated the formation of small spherical Ag NPs in stabilizer with mean size 4 nm in diameter. The size of the Ag NPs into MMT is smaller than that of the synthesized Ag NPs in absence of MMT (30 nm). This is due to the availability of more nucleating sites offered by MMT matrix.

The results of inhibition zones for all samples indicated that the MMT clay and Ag-MMT nanocomposite showed no antibacterial activity, but the action Ag NPs was more than them (Fig. 4). Because of their size, Ag NPs can easily reach the nuclear content of bacteria and they present a large and impressive surface area, enabling broad contact with bacteria [19]. For solid support systems, some researchers have argued that Ag^+ ions released from the surface of Ag NPs are responsible for their antibacterial activity [19].The results revealed that the Ag NPs in MMT indicated no antibacterial activity. Probably, Ag NPs were very stable in MMT matrix and not oxidatively released Ag ions from NPs surface when the Ag-MMT interacts with an aqueous phase.

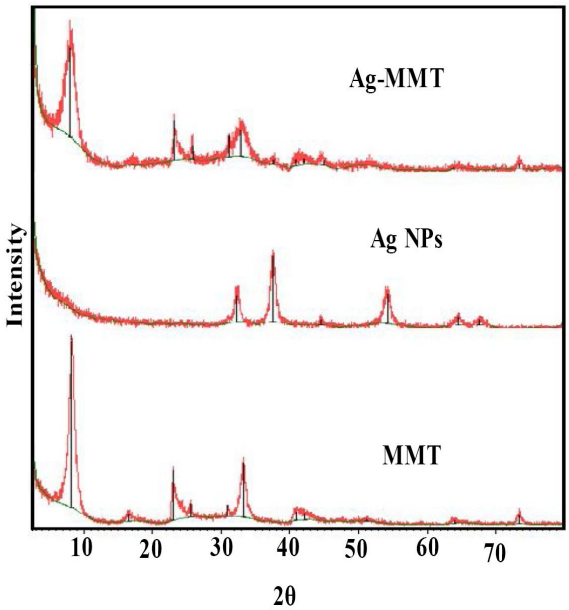

Fig. 1. XRD patterns of MMT, Ag NPs and Ag-MMT nanocomposite.

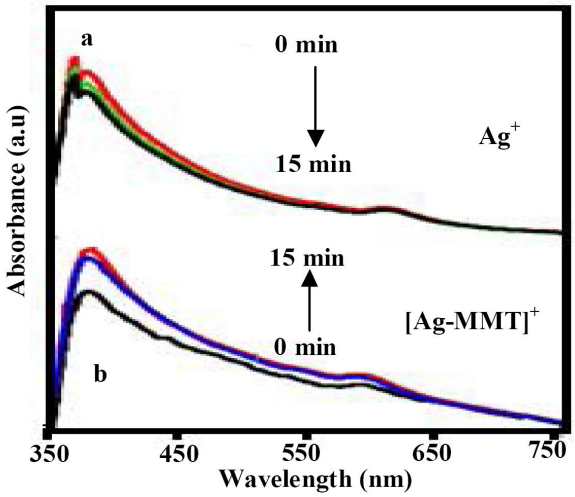

Fig. 2. UV–Vis spectra of the (a) silver nitrate solution and the (b) $[Ag\text{-}MMT]^+$ suspension with *Urtic*a leaf extract recorded as a function of time. Concentration of $AgNO_3$: 1 mM.

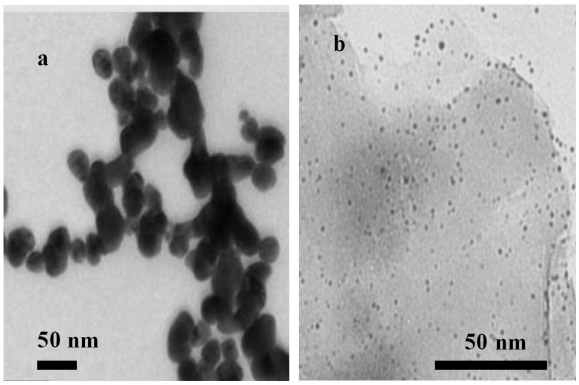

Fig. 3. TEM images of (a) Ag NPs, (b) Ag-MMT nanocomposite.

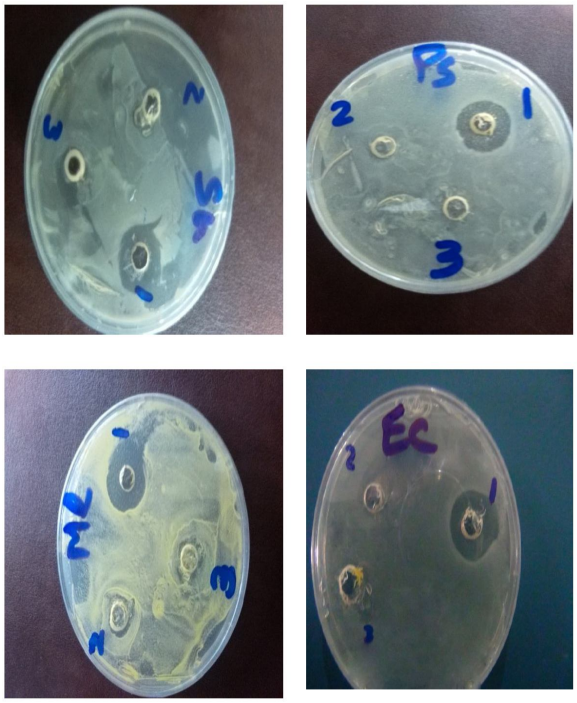

Fig. 4. Comparison of the inhibition zone test between Gram-negative and Gram-positive bacteria. 1- Ag NPs, 2- Ag-MMT nanocomposite and 3- MMT stabilizer

CONCLUSIONS

In summary, Ag NPs was incorporated in MMT matrix by the simple green method. *Urtica dioica* leaf extract were used as a reducing agent. The formation of Ag NPs in clay was observed by TEM, XRD, FT-IR and UV-Vis. The support had an important role in the stability, particle size and aggregation of the Ag NPs. Comparison of the antibacterial activity of synthesized samples clearly indicated that the Ag NPs had the best antibacterial activity for the inhibition of bacterial growth with respect to Ag-MMT nanocomposite.

REFERENCES

[1] H. Barani, M. Montazer, N. Samadi, T. Toliyat, In Situ synthsis of Nano Silver/Lecithin on Wool: Enhancing Nanoparticles Diffusion",Colloid Surf., B vol. 92, pp. 9–15, 2012.

[2] W. Zhou, Y. Ma, H. Yang, Y. Ding, X. Luo, A label-free biosensor based on silver nanoparticles array for clinical detection of serum p53 in head and neck squamous cell carcinoma",Int. J. Nanomed, vol. 6, pp. 381–386, 2011.

[3] D.A. Giljohann, D.S. Seferos, W.L. Daniel, M.D. Massich, P.C. Patel, C.A. Mirkin, Gold nanoparticles for biology and medicine", Angew. Chem. Int. Ed, vol. 49, pp. 3280–3294, 2010.

[4] J. Luo, S. Jiang, H. Zhang, J. Jiang, X. Liu, A novel non-enzymatic glucose sensor based on Cu nanoparticle modified graphene sheets electrode", Anal. Chim. Acta, vol. 709, pp. 47–53, 2012.

[5] S. Sundarrajan, A. Richard Chandrasekaran, S. Ramakrishna, An Update on Nanomaterials-Based Textiles for Protection and Decontamination",J. Am. Ceram. Soc, vol. 93, pp. 3955–3975, 2010.

[6] V.C. Verma, R.N. Kharwar, A.C. Gange, Biosynthesis of antimicrobial silver nanoparticles by the endophytic fungus. Aspergillus clavatus", Nanomedicine, vol. 5, pp. 33–40, 2010.

[7] I. Willner, R. Baron, B. Willner, Growing Metal Nanoparticles by Enzymes", Adv. Mater, vol.18, pp. 1109-1120, 2006.

[8] G. Zhan, J. Huang, M. Du, I. Abdul-Rauf, Y. Ma, Q. Li, Green synthesis of Au–Pd bimetallic nanoparticles: Single-step bioreduction method with plant extract", Mater. Lett, vol. 65, pp. 2989–2991, 2011.

[9] M.A.G. Maobe, R.M. Nyarango, Fourier Transformer Infra-Red Spectrophotometer Analysis of Urtica dioica Medicinal Herb Used for the Treatment of Diabetes, Malaria and Pneumonia in Kisii Region",World. Appl. Sci. J, vol. 21, pp. 1128-1135, 2013.

[10] P. Radhika, B.S. Sastry, B.M. Harica, Antimicrobial screening of Andrographis paniculata (Acanthaceae) root extracts",Res. J. Biotechnol, vol. 3, pp. 62–63, 2008.

[11] R-M. Torres Sanchez, M-J. Genet, E-M. Gaigneaux, M. Dos Santos Afonso, S. Yunes, Appl Clay Sci 53 (2007) 366–373

[12] H. Dong, G. Chen, J. Sun, Ch. Li, Y. Yu, D. Chen, A novel high-efficiency visible-light sensitive Ag_2CO_3 photocatalyst with universal photodegradation performance: simple synthesis, reactionmechanismand first-principles study", Appl. Catal., B, vol. 134-135, pp. 46-54, 2013.

[13] W. J. Zhou, Y. H. Leng, D. M. Hou, H. D. Li, L. G. Li, G. Q. Li, H. Liu and S. W. Chen, A novel high-efficiency visible-light sensitive Ag_2CO_3 photocatalyst with universal photodegradation performance: simple

synthesis, reactionmechanismand first-principles study", Nanoscale, vol. 6, pp. 4698-4703, 2014.
[14] V.C. Farmer, J.D. Russell, Effect of particle size and structure on the vibrational frequencies of layer silicates", Spectrochimica Acta, vol.22, pp. 389-398, 1966.
[15] S. Shiv Shankar, A. Ahmad, M. Sastry, Geranium leaf assisted biosynthesis of silver nanoparticles", Biotechnol. Prog, vol. 19, pp. 1627-1631, 2003.
[16] K.C. Song, S.M. Lee, T.S. Park, B.S. Lee, Preparation of colloidal silver nanoparticles by chemical reduction method", Korean J. Chem. Eng, vol. 26, pp. 153–155, 2009.
[17] K. Patel, S. Kapoor, D.P. Dave, T. Mukherjee, Synthesis of nanosized silver colloids by microwave dielectric heating", J. Chem. Sci, vol. 117, pp. 53–60, 2005.
[18] M. Moritz, M. Geszke-Moritz, The newest achievements in synthesis, immobilization and practical applications of antibacterial nanoparticles", Chem. Eng. J, vol. 228, pp. 596–613, 2013.
[19] T. Pandiyarajan, R. Udayabhaskar, S. Vignesh, R. Arthur James, B. Karthikeyan, Synthesis and concentration dependent antibacterial activities of CuO nanoflakes", Mater. Sci. Eng., C vol. 33, pp. 2020–2024, 2013.

★★★